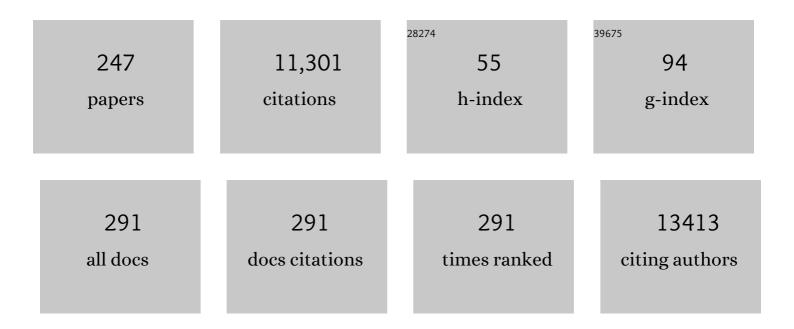
## **Richard I Walton**

List of Publications by Year in descending order

Source: https://exaly.com/author-pdf/2253699/publications.pdf Version: 2024-02-01



#	Article	IF	CITATIONS
1	Enhanced stability and efficiency in hole-transport-layer-free CsSnI3 perovskite photovoltaics. Nature Energy, 2016, 1, .	39.5	491
2	Time-resolved in situ X-ray diffraction study of the liquid-phase reconstruction of Mg–Al–carbonate hydrotalcite-like compounds. Journal of Materials Chemistry, 2000, 10, 1713-1720.	6.7	347
3	Subcritical solvothermal synthesis of condensed inorganic materials. Chemical Society Reviews, 2002, 31, 230-238.	38.1	344
4	ElAM: A computer program for the analysis and representation of anisotropic elastic properties. Computer Physics Communications, 2010, 181, 2102-2115.	7.5	321
5	Structures of Uncharacterised Polymorphs of Gallium Oxide from Total Neutron Diffraction. Chemistry - A European Journal, 2013, 19, 2803-2813.	3.3	316
6	Solvothermal synthesis of perovskites and pyrochlores: crystallisation of functional oxides under mild conditions. Chemical Society Reviews, 2010, 39, 4303.	38.1	300
7	Effect of the nature of the metal on the breathing steps in MOFs with dynamic frameworks. Chemical Communications, 2008, , 4732.	4.1	274
8	Water‧plitting Electrocatalysis in Acid Conditions Using Ruthenateâ€Iridate Pyrochlores. Angewandte Chemie - International Edition, 2014, 53, 10960-10964.	13.8	193
9	Timeâ€Resolved In Situ Diffraction Study of the Solvothermal Crystallization of Some Prototypical Metal–Organic Frameworks. Angewandte Chemie - International Edition, 2010, 49, 763-766.	13.8	192
10	Structural Effects of Solvents on the Breathing of Metal–Organic Frameworks: An In Situ Diffraction Study. Angewandte Chemie - International Edition, 2008, 47, 4100-4105.	13.8	189
11	Tin perovskite/fullerene planar layer photovoltaics: improving the efficiency and stability of lead-free devices. Journal of Materials Chemistry A, 2015, 3, 11631-11640.	10.3	188
12	Efficient Separation of Terephthalate and Phthalate Anions by Selective Ion-Exchange Intercalation in the Layered Double Hydroxide Ca2Al(OH)6·NO3·2H2O. Chemistry of Materials, 2000, 12, 1990-1994.	6.7	175
13	display="inline"> <mmi:mi>K</mmi:mi> CrO <mmi:math xmlns:mml="http://www.w3.org/1998/Math/MathML" display="inline"&gt;<mml:msub><mml:mrow< td=""><td></td><td></td></mml:mrow<></mml:msub></mmi:math 		

#	Article	IF	CITATIONS
19	Nanoparticulate Palladium Supported by Covalently Modified Silicas:  Synthesis, Characterization, and Application as Catalysts for the Suzuki Coupling of Aryl Halides. Chemistry of Materials, 2005, 17, 701-707.	6.7	131
20	A time-resolved diffraction study of a window of stability in the synthesis of a copper carboxylate metal–organic framework. CrystEngComm, 2011, 13, 103-108.	2.6	130
21	Tuning the breathing behaviour of MIL-53 by cation mixing. Chemical Communications, 2012, 48, 10237.	4.1	129
22	An in Situ Energy-Dispersive X-ray Diffraction Study of the Hydrothermal Crystallization of Zeolite A. 1. Influence of Reaction Conditions and Transformation into Sodalite. Journal of Physical Chemistry B, 2001, 105, 83-90.	2.6	121
23	Watching solids crystallise using in situ powder diffraction. Chemical Communications, 2000, , 2283-2291.	4.1	116
24	Natrolite: A zeolite with negative Poisson's ratios. Journal of Applied Physics, 2007, 101, 086102.	2.5	107
25	Characterization of Structural Disorder in γ-Ga <sub>2</sub> O <sub>3</sub> . Journal of Physical Chemistry C, 2014, 118, 16188-16198.	3.1	107
26	Bismuth Iridium Oxide Oxygen Evolution Catalyst from Hydrothermal Synthesis. Chemistry of Materials, 2012, 24, 4192-4200.	6.7	106
27	Selective Sorption of Organic Molecules by the Flexible Porous Hybrid Metalâ^'Organic Framework MIL-53(Fe) Controlled by Various Hostâ^'Guest Interactions. Chemistry of Materials, 2010, 22, 4237-4245.	6.7	104
28	Mixedâ€Metal MILâ€100(Sc,M) (M=Al, Cr, Fe) for Lewis Acid Catalysis and Tandem CC Bond Formation and Alcohol Oxidation. Chemistry - A European Journal, 2014, 20, 17185-17197.	3.3	104
29	Instant MOFs: continuous synthesis of metal–organic frameworks by rapid solvent mixing. Chemical Communications, 2012, 48, 10642.	4.1	103
30	Effect of Phase Junction Structure on the Photocatalytic Performance in Overall Water Splitting: Ga <sub>2</sub> O <sub>3</sub> Photocatalyst as an Example. Journal of Physical Chemistry C, 2015, 119, 18221-18228.	3.1	101
31	Structure and NMR assignment in calcined and as-synthesized forms of AlPO-14: a combined study by first-principles calculations and high-resolution 27Al–31P MAS NMR correlation. Physical Chemistry Chemical Physics, 2008, 10, 5754.	2.8	95
32	A study of the manganites La0.5M0.5MnO3(M = Ca, Sr, Ba) prepared by hydrothermal synthesis. Journal of Materials Chemistry, 2005, 15, 1542.	6.7	94
33	23Na multiple-quantum MAS NMR of the perovskites NaNbO3and NaTaO3. Physical Chemistry Chemical Physics, 2006, 8, 3423-3431.	2.8	86
34	MILâ€53 and its Isoreticular Analogues: a Review of the Chemistry and Structure of a Prototypical Flexible Metalâ€Organic Framework. Israel Journal of Chemistry, 2018, 58, 1019-1035.	2.3	82
35	Methods for the synthesis of large crystals of silicate zeolites. Microporous and Mesoporous Materials, 2005, 79, 339-352.	4.4	81
36	Tuning the properties of the UiO-66 metal organic framework by Ce substitution. Chemical Communications, 2015, 51, 14458-14461.	4.1	79

#	Article	IF	CITATIONS
37	Brillouin scattering study on the single-crystal elastic properties of natrolite and analcime zeolites. Journal of Applied Physics, 2005, 98, 053508.	2.5	76
38	Conformation-Controlled Sorption Properties and Breathing of the Aliphatic Al-MOF [Al(OH)(CDC)]. Inorganic Chemistry, 2014, 53, 4610-4620.	4.0	74
39	Dynamics on the Microsecond Timescale in Microporous Aluminophosphate AlPO-14 as Evidenced by27Al MQMAS and STMAS NMR Spectroscopy. Journal of the American Chemical Society, 2006, 128, 8054-8062.	13.7	72
40	Ruthenium(V) Oxides from Lowâ€Temperature Hydrothermal Synthesis. Angewandte Chemie - International Edition, 2014, 53, 4423-4427.	13.8	70
41	Towards scalable and controlled synthesis of metal–organic framework materials using continuous flow reactors. Reaction Chemistry and Engineering, 2016, 1, 352-360.	3.7	68
42	Localized Structural Alterations Underlying a Subset of Unexplained Sudden Cardiac Death. Circulation: Arrhythmia and Electrophysiology, 2018, 11, e006120.	4.8	67
43	Hydrothermal Synthesis of (C6N2H14)2(UVI2UIVO4F12), a Mixed-Valent One-Dimensional Uranium Oxyfluoride. Inorganic Chemistry, 2000, 39, 3791-3798.	4.0	65
44	Control of polymorphism in NaNbO3by hydrothermal synthesis. Chemical Communications, 2009, , 68-70.	4.1	65
45	Exceptionally Efficient and Recyclable Heterogeneous Metal–Organic Framework Catalyst for Glucose Isomerization in Water. ChemCatChem, 2018, 10, 706-709.	3.7	65
46	lsomorphous Substitution in a Flexible Metal–Organic Framework: Mixed-Metal, Mixed-Valent MIL-53 Type Materials. Inorganic Chemistry, 2013, 52, 8171-8182.	4.0	64
47	Yb <sub>3</sub> O(OH) <sub>6</sub> Cl·2H <sub>2</sub> O: An Anion-Exchangeable Hydroxide with a Cationic Inorganic Framework Structure. Journal of the American Chemical Society, 2010, 132, 13618-13620.	13.7	63
48	Subcritical Hydrothermal Synthesis of Perovskite Manganites:Â A Direct and Rapid Route to Complex Transition-Metal Oxides. Chemistry of Materials, 2003, 15, 1401-1403.	6.7	62
49	In Situ Investigation of the Thermal Decomposition of Ammonium Tetrathiomolybdate Using Combined Time-Resolved X-ray Absorption Spectroscopy and X-ray Diffraction. Chemistry of Materials, 1998, 10, 3737-3745.	6.7	61
50	Synthesis, Structures, and Reactivity of Two Compounds Containing the Tancoite-like [Ga(HPO4)2F]2-â^žChain. Chemistry of Materials, 2000, 12, 1977-1984.	6.7	60
51	Off-Axis Elastic Properties and the Effect of Extraframework Species on Structural Flexibility of the NAT-Type Zeolites:A Simulations of Structure and Elastic Properties. Chemistry of Materials, 2007, 19, 2423-2434.	6.7	59
52	Perovskite Oxides Prepared by Hydrothermal and Solvothermal Synthesis: A Review of Crystallisation, Chemistry, and Compositions. Chemistry - A European Journal, 2020, 26, 9041-9069.	3.3	59
53	An in Situ Energy-Dispersive X-ray Diffraction Study of the Hydrothermal Crystallizations of Open-Framework Gallium Oxyfluorophosphates with the ULM-3 and ULM-4 Structures. Chemistry of Materials, 1999, 11, 3201-3209.	6.7	58
54	The room-temperature crystallisation of a one-dimensional gallium fluorophosphate, Ga(HPO4)2F·H3N(CH2)3NH3·2H2O, a precursor to three-dimensional microporous gallium fluorophosphates. Chemical Communications, 2000, , 203-204.	4.1	58

#	Article	IF	CITATIONS
55	Efficient separation of pyridinedicarboxylates by preferential anion exchange intercalation in [LiAl2(OH)6]Cl·H2O. Journal of Materials Chemistry, 2000, 10, 1881-1886.	6.7	58
56	Cerium(III) and Cerium(IV) Bis(η8-pentalene) Sandwich Complexes: Synthetic, Structural, Spectroscopic, and Theoretical Studies. Organometallics, 2007, 26, 3111-3119.	2.3	57
57	Synthesis and characterisation of the first three-dimensional framework cobalt–gallium phosphate [C5H5NH]+[CoGa2P3O12]–. Journal of the Chemical Society Chemical Communications, 1994, , 2453-2454.	2.0	54
58	On the advantages of the use of the three-element detector system for measuring EDXRD patterns to follow the crystallisation of open-framework structures. Physical Chemistry Chemical Physics, 2000, 2, 3523-3527.	2.8	54
59	Separation of nucleoside monophosphates using preferential anion exchange intercalation in layered double hydroxides. Solid State Sciences, 2001, 3, 883-886.	3.2	54
60	lodine sequestration by thiol-modified MIL-53(Al). CrystEngComm, 2016, 18, 8108-8114.	2.6	54
61	Solvothermal synthesis of cerium oxides. Progress in Crystal Growth and Characterization of Materials, 2011, 57, 93-108.	4.0	53
62	Inâ€Situ Observation of Successive Crystallizations and Metastable Intermediates in the Formation of Metal–Organic Frameworks. Angewandte Chemie - International Edition, 2016, 55, 2012-2016.	13.8	53
63	Crystallisation Kinetics of Metal Organic Frameworks From <i>in situ</i> Time-Resolved X-ray Diffraction, 2013, 28, S256-S275.	0.2	52
64	Direct in situ observation of increasing structural dimensionality during the hydrothermal formation of open-framework zinc phosphates. Chemical Communications, 2001, , 1990-1991.	4.1	51
65	In situ Fe XAFS of reversible lithium insertion in a flexible metal organic framework material. Electrochemistry Communications, 2009, 11, 1881-1884.	4.7	51
66	Electrical semiconduction modulated by light in a cobalt and naphthalene diimide metal-organic framework. Nature Communications, 2017, 8, 2139.	12.8	51
67	93Nb NMR and DFT investigation of the polymorphs of NaNbO3. Physical Chemistry Chemical Physics, 2011, 13, 7565.	2.8	50
68	Structures and Magnetism of the Rare-Earth Orthochromite Perovskite Solid Solution La <sub><i>x</i></sub> Sm <sub>1–<i>x</i></sub> CrO <sub>3</sub> . Inorganic Chemistry, 2013, 52, 12161-12169.	4.0	50
69	An NMR crystallography study of the hemihydrate of 2′, 3′-O-isopropylidineguanosine. Solid State Nuclear Magnetic Resonance, 2015, 65, 41-48.	2.3	48
70	Probing Molten Salt Flux Reactions Using Time-Resolved in Situ High-Temperature Powder X-ray Diffraction:  A New Synthesis Route to the Mixed-Valence NaTi2O4. Chemistry of Materials, 2004, 16, 1153-1159.	6.7	45
71	Adsorption of N/S heterocycles in the flexible metal–organic framework MIL-53(FeIII) studied by in situ energy dispersive X-ray diffraction. Physical Chemistry Chemical Physics, 2013, 15, 8606.	2.8	44
72	Quantification of the Transmural Dynamics of Atrial Fibrillation by Simultaneous Endocardial and Epicardial Optical Mapping in an Acute Sheep Model. Circulation: Arrhythmia and Electrophysiology, 2015, 8, 456-465.	4.8	44

#	Article	IF	CITATIONS
73	Hydrothermal synthesis of the perovskite manganites Pr0.5Sr0.5MnO3 and Nd0.5Sr0.5MnO3 and alkali-earth manganese oxides CaMn2O4, 4H-SrMnO3, and 2H-BaMnO3. Journal of Solid State Chemistry, 2005, 178, 1683-1691.	2.9	43
74	Rapid and reversible formation of a crystalline hydrate of a metal–organic framework containing a tube of hydrogen-bonded water. Chemical Communications, 2011, 47, 713-715.	4.1	43
75	Antiferromagnetism atT>500Kin the layered hexagonal ruthenateSrRu2O6. Physical Review B, 2015, 92, .	3.2	43
76	Following the hydrothermal crystallisation of zeolites using time-resolved in situ powder neutron diffraction. Microporous and Mesoporous Materials, 2001, 48, 79-88.	4.4	42
77	Uptake of Liquid Alcohols by the Flexible Fe <sup>III</sup> Metal–Organic Framework MILâ€53 Observed by Timeâ€Resolved In Situ Xâ€ray Diffraction. Chemistry - A European Journal, 2011, 17, 7069-7079.	3.3	42
78	Local Order of Amorphous Zeolite Precursors from 29Si{H} CPMAS and 27Al and 23Na MQMAS NMR and Evidence for the Nature of Medium-Range Order from Neutron Diffraction. Journal of Physical Chemistry B, 2004, 108, 8208-8217.	2.6	41
79	Exchange of Coordinated Solvent During Crystallization of a Metal–Organic Framework Observed by In Situ Highâ€Energy Xâ€ray Diffraction. Angewandte Chemie - International Edition, 2016, 55, 4992-4996.	13.8	41
80	Negative Poisson's ratios in siliceous zeolite MFI-silicalite. Journal of Chemical Physics, 2008, 128, 184503.	3.0	40
81	Transformation of AlPO-53 to JDF-2: Reversible Dehydration of a Templated Aluminophosphate Studied by MAS NMR and Diffraction. Journal of Physical Chemistry C, 2009, 113, 10780-10789.	3.1	40
82	Incorporation of square-planar Pd <sup>2+</sup> in fluorite CeO <sub>2</sub> : hydrothermal preparation, local structure, redox properties and stability. Journal of Materials Chemistry A, 2015, 3, 13072-13079.	10.3	40
83	Synthesis and Luminescent Properties of REVO <sub>4</sub> –REPO <sub>4</sub> (RE = Y, Eu, Gd, Er, Tm,) Tj E Journal of Physical Chemistry C, 2015, 119, 24062-24074.	TQq1 1 0 3.1	.784314 rg 40
84	Nanocrystalline Ceriumâ^'Bismuth Oxides: Synthesis, Structural Characterization, and Redox Properties. Chemistry of Materials, 2010, 22, 6191-6201.	6.7	39
85	Negative Thermal Expansion in the Aluminum and Gallium Phosphate Zeotypes with CHA and AEI Structure types. Chemistry of Materials, 2009, 21, 3380-3390.	6.7	38
86	Novel apparatus for the in situ study of hydrothermal crystallizations using time-resolved neutron diffraction. Review of Scientific Instruments, 1999, 70, 3391-3396.	1.3	37
87	Synthesis, Structure, and Crystallization Study of a Layered Lithium Thiophene-Dicarboxylate. Crystal Growth and Design, 2012, 12, 1531-1537.	3.0	37
88	The flexibility of modified-linker MIL-53 materials. Dalton Transactions, 2016, 45, 4162-4168.	3.3	37
89	[C9H20N][Al2(HPO4)2(PO4)]: An Aluminium Phosphate with a New Layer Topology. Journal of Solid State Chemistry, 1999, 145, 731-738.	2.9	36
90	Crystallization of a Large-Pore Three-Dimensional Gallium Fluorophosphate under Mild Conditions. Angewandte Chemie - International Edition, 2000, 39, 4552-4555.	13.8	36

#	Article	IF	CITATIONS
91	Structural, spectroscopic, magnetic and electrical characterization of Ca-doped polycrystalline bismuth ferrite, Bi <sub>1â^'<i>x</i></sub> Ca <sub><i>x</i></sub> FeO <sub>3â´'<i>x</i>/2</sub> ( <i>x</i> â‰)#Tj	ET&Qq1 i	1 <b>037</b> 84314 rg
92	A highly active and synergistic Pt/Mo2C/Al2O3 catalyst for water-gas shift reaction. Molecular Catalysis, 2018, 455, 38-47.	2.0	36
93	Thermal transformations of Cu–Mg (Zn)–Al(Fe) hydrotalcite-like materials into metal oxide systems and their catalytic activity in selective oxidation of ammonia to dinitrogen. Journal of Thermal Analysis and Calorimetry, 2013, 114, 731-747.	3.6	35
94	Replacement of Chromium by Non-Toxic Metals in Lewis-Acid MOFs: Assessment of Stability as Glucose Conversion Catalysts. Catalysts, 2019, 9, 437.	3.5	35
95	Synthesis and Structure of Low-Dimensional Gallium Fluorodiphosphates Seen during the Crystallization of the Three-Dimensional Microporous Gallium Fluorophosphate ULM-3. Chemistry of Materials, 2002, 14, 4448-4459.	6.7	34
96	Porous Metal–Organic Frameworks for Enhanced Performance Silicon Anodes in Lithium-Ion Batteries. Chemistry of Materials, 2019, 31, 4156-4165.	6.7	34
97	An in Situ Energy-Dispersive X-ray Diffraction Study of the Hydrothermal Crystallization of Zeolite A. 2. Effect of Deuteration on Crystallization Kinetics. Journal of Physical Chemistry B, 2001, 105, 91-96.	2.6	33
98	Direct, static measurement of single-crystal Young's moduli of the zeolite natrolite: Comparison with dynamic studies and simulations. Acta Materialia, 2006, 54, 2533-2545.	7.9	33
99	Recent results from the in situ study of hydrothermal crystallisations using time-resolved X-ray and neutron diffraction methods. Faraday Discussions, 2003, 122, 331-341.	3.2	32
100	Pair Distribution Function Analysis of Structural Disorder by Nb <sup>5+</sup> Inclusion in Ceria: Evidence for Enhanced Oxygen Storage Capacity from Under-Coordinated Oxide. Journal of the American Chemical Society, 2018, 140, 1588-1591.	13.7	32
101	A hydrothermally stable ytterbium metal–organic framework as a bifunctional solid-acid catalyst for glucose conversion. Chemical Communications, 2019, 55, 11446-11449.	4.1	32
102	Hydrothermal synthesis map of bismuth titanates. Journal of Solid State Chemistry, 2012, 189, 32-37.	2.9	31
103	Cs <sub>1â^'x</sub> Rb <sub>x</sub> SnI <sub>3</sub> light harvesting semiconductors for perovskite photovoltaics. Materials Chemistry Frontiers, 2018, 2, 1515-1522.	5.9	31
104	Low-temperature wet chemistry synthetic approaches towards ferrites. Inorganic Chemistry Frontiers, 2020, 7, 3282-3314.	6.0	31
105	Electric Field ontrolled Synthesis and Characterisation of Single Metal–Organicâ€Framework (MOF) Nanoparticles. Angewandte Chemie - International Edition, 2020, 59, 19696-19701.	13.8	31
106	Amorphous MoS3: clusters or chains? The structural evidence. Journal of Non-Crystalline Solids, 1998, 232-234, 434-439.	3.1	30
107	Two chain gallium fluorodiphosphates: synthesis, structure solution, and their transient presence during the hydrothermal crystallisation of a microporous gallium fluorophosphateElectronic supplementary information (ESI) available: crystal data, atomic coordinates and metrical data for 1 and 2. See http://www.rsc.org/suppdata/cc/b2/b201178f/. Chemical Communications. 2002 826-827.	4.1	30
108	Ag2CuMnO4: A new silver copper oxide with delafossite structure. Journal of Solid State Chemistry, 2006, 179, 3883-3892.	2.9	29

#	Article	IF	CITATIONS
109	A lithium–organic framework with coordinatively unsaturated metal sites that reversibly binds water. Chemical Communications, 2012, 48, 10639.	4.1	29
110	Composition of eye cosmetics (kohls) used in Cairo. International Journal of Environmental Health Research, 2004, 14, 83-91.	2.7	28
111	M(ii) (M = Mn, Co, Ni) variants of the MIL-53-type structure with pyridine-N-oxide as a co-ligand. CrystEngComm, 2013, 15, 9679.	2.6	28
112	Synthesis and Polymorphism of Mixed Aluminum–Gallium Oxides. Inorganic Chemistry, 2020, 59, 3805-3816.	4.0	28
113	Synthesis and structure of a novel open-framework gallium phosphate [Me2NH(CH2)2NHMe2]2+[Ga4P5O2OH]2–·H2O. Journal of the Chemical Society Chemical Communications, 1995, .	2.0	27
114	Oneâ€Step Hydrothermal Synthesis of Nanocrystalline Ceriaâ€Zirconia Mixed Oxides: The Beneficial Effect of Sodium Inclusion on Redox Properties. Advanced Materials, 2007, 19, 4500-4504.	21.0	27
115	Chirality and diastereoselection in the μ-oxo diiron complexes L2Fe–O–FeL2 (L = bidentate) Tj ETQq1 1 0.78	34314 rgB	T /Overlock 27
116	Control of chemical state of cerium in doped anatase TiO <sub>2</sub> by solvothermal synthesis and its application in photocatalytic water reduction. Journal of Materials Chemistry A, 2015, 3, 9890-9898.	10.3	27
117	Systematic Modification of UiOâ€66 Metalâ€Organic Frameworks for Glucose Conversion into 5â€Hydroxymethyl Furfural in Water. ChemCatChem, 2021, 13, 2517-2529.	3.7	26
118	Transmural electrophysiological heterogeneity, the T-wave and ventricular arrhythmias. Progress in Biophysics and Molecular Biology, 2016, 122, 202-214.	2.9	25
119	Controlling the crystallisation of oxide materials by solvothermal chemistry: tuning composition, substitution and morphology of functional solids. CrystEngComm, 2016, 18, 7656-7670.	2.6	25
120	A Multinuclear NMR Study of Six Forms of AlPO-34: Structure and Motional Broadening. Journal of Physical Chemistry C, 2017, 121, 1781-1793.	3.1	25
121	Local structures of the amorphous chromium sulfide, CrS3, and selenide, CrSe3, from X-ray absorption studies. Journal of the Chemical Society Dalton Transactions, 1996, , 2245.	1.1	24
122	A Multinuclear Solid-State NMR Study of Templated and Calcined Chabazite-Type GaPO-34. Journal of Physical Chemistry C, 2012, 116, 15048-15057.	3.1	24
123	Interaction of methanol with the flexible metal-organic framework MIL-53(Fe) observed by inelastic neutron scattering. Chemical Physics, 2013, 427, 30-37.	1.9	24
124	23-Electron Octahedral Molybdenum Cluster Complex [{Mo6I8}Cl6]â^'. Inorganic Chemistry, 2018, 57, 811-820.	4.0	24
125	Hierarchically Structured Ceria-Silica: Synthesis and Thermal Properties. Journal of Physical Chemistry C, 2012, 116, 13435-13445.	3.1	23
126	Comparison of techniques for the synthesis of hydroxyapatite. Bioinspired, Biomimetic and Nanobiomaterials, 2015, 4, 37-47.	0.9	23

#	Article	IF	CITATIONS
127	Elucidating the role of the hole-extracting electrode on the stability and efficiency of invertedACsSnI <sub>3</sub> /C <sub>60</sub> perovskite photovoltaics. Journal of Materials Chemistry A, 2017, 5, 21836-21845.	10.3	23
128	Highly Selective Continuous Flow Hydrogenation of Cinnamaldehyde to Cinnamyl Alcohol in a Pt/SiO2 Coated Tube Reactor. Catalysts, 2018, 8, 58.	3.5	23
129	High Conductivity in Hydrothermally Grown AgCuO <sub>2</sub> Single Crystals Verified Using Focused-Ion-Beam-Deposited Nanocontacts. Inorganic Chemistry, 2010, 49, 10977-10983.	4.0	22
130	Structural variety in iridate oxides and hydroxides from hydrothermal synthesis. Chemical Science, 2011, 2, 1573.	7.4	22
131	Inference of oxygen vacancies in hydrothermal Na0.5Bi0.5TiO3. Applied Physics Letters, 2012, 101, 142902.	3.3	22
132	A multiple-quantum 23Na MAS NMR study of amorphous sodium gallium silicate zeolite precursors. Journal of Materials Chemistry, 2002, 12, 1469-1474.	6.7	21
133	Hydrothermal Synthesis of a Cerium(IV) Pyrochlore with Low-Temperature Redox Properties. Angewandte Chemie - International Edition, 2006, 45, 2442-2446.	13.8	21
134	Low-Temperature Redox Properties of Nanocrystalline Cerium (IV) Oxides Revealed by in Situ XANES. Journal of Physical Chemistry C, 2007, 111, 14035-14039.	3.1	21
135	A combined in situ X-ray absorption spectroscopy and X-ray diffraction study of the thermal decomposition of ammonium tetrathiotungstate. Journal of Materials Chemistry, 1999, 9, 1347-1355.	6.7	20
136	An analytical model for producing negative Poisson's ratios and its application in explaining off-axis elastic properties of the NAT-type zeolites. Acta Materialia, 2007, 55, 5697-5707.	7.9	20
137	Metastable (Bi, M) <sub>2</sub> (Fe, Mn, Bi) <sub>2</sub> O <sub>6+<i>x</i></sub> (M = Na or K) Pyrochlores from Hydrothermal Synthesis. Inorganic Chemistry, 2014, 53, 13197-13206.	4.0	20
138	Air and moisture stable covalently-bonded tin( <scp>ii</scp> ) coordination polymers. Dalton Transactions, 2018, 47, 8013-8022.	3.3	20
139	Metal–Organic Frameworks from Divalent Metals and 1,4-Benzenedicarboxylate with Bidentate Pyridine- <i>N</i> -oxide Co-ligands. Crystal Growth and Design, 2015, 15, 891-899.	3.0	19
140	Location of CO <sub>2</sub> during its uptake by the flexible porous metal–organic framework MIL-53(Fe): a high resolution powder X-ray diffraction study. CrystEngComm, 2015, 17, 422-429.	2.6	19
141	High energy X-rays for following metal-organic framework formation: Identifying intermediates in interpenetrated MOF-5 crystallisation. Microporous and Mesoporous Materials, 2017, 254, 178-183.	4.4	19
142	Ambient temperature crystallisation of a lamellar gallium fluorophosphate from the synthesis solution of microporous ULM-5. Chemical Communications, 2001, , 994-995.	4.1	18
143	An Investigation of the Synthesis of the Layered Perovskite RbCa2Nb3O10 Using Time-Resolved in Situ High-Temperature Powder X-ray Diffraction. Chemistry of Materials, 2002, 14, 4343-4349.	6.7	18
144	The bulk material dissolution method with small amines for the synthesis of large crystals of the siliceous zeolites ZSM-22 and ZSM-48. Microporous and Mesoporous Materials, 2009, 119, 259-266.	4.4	18

#	Article	IF	CITATIONS
145	Investigation of Hydrothermal Routes to Mixed-Metal Cerium Titanium Oxides and Metal Oxidation State Assignment Using XANES. Inorganic Chemistry, 2004, 43, 2189-2196.	4.0	17
146	Dissolution Kinetics of Polycrystalline Calcium Sulfate-Based Materials: Influence of Chemical Modification. ACS Applied Materials & amp; Interfaces, 2011, 3, 3528-3537.	8.0	17
147	(M,Ru)O <sub>2</sub> (M = Mg, Zn, Cu, Ni, Co) Rutiles and Their Use as Oxygen Evolution Electrocatalysts in Membrane Electrode Assemblies under Acidic Conditions. Chemistry of Materials, 2020, 32, 6150-6160.	6.7	17
148	An X-ray absorption fine structure study of amorphous precursors of a gallium silicate zeolite. Journal of Physics and Chemistry of Solids, 2001, 62, 1469-1479.	4.0	16
149	Polymorphism and variable structural dimensionality in the iron(III) phosphate oxalate system: a new polymorph of 3D [Fe2(HPO4)2(C2O4)(H2O)2]·2H2O and the layered material [Fe2(HPO4)2(C2O4)(H2O)2]. Dalton Transactions, 2009, , 9176.	3.3	16
150	Heterobimetallic Sodium–Lithium Based Metal–Organic Framework Showing the βâ€Cristobalite Topology and Having High Permanent Porosity. European Journal of Inorganic Chemistry, 2013, 2013, 1138-1141.	2.0	16
151	An XRD and NMR crystallographic investigation of the structure of 2,6-lutidinium hydrogen fumarate. CrystEngComm, 2019, 21, 3502-3516.	2.6	16
152	Sulfur–sulfur bonding in the amorphous sulfides WS3, WS5, and Re2S7 from sulfur K-edge EXAFS studies. Journal of the Chemical Society Dalton Transactions, 1999, , 2877-2883.	1.1	15
153	Preparation, structural diversity and characterization of a family of Cd(ii)–organic frameworks. Dalton Transactions, 2013, 42, 12468.	3.3	15
154	Spontaneous formation of circular and vortex ferroelectric domain structure in hexagonal YMnO3 and YMn0.9Fe0.1O3 prepared by low temperature solution synthesis. Applied Physics Letters, 2015, 107, .	3.3	15
155	Inâ€Situ Observation of Successive Crystallizations and Metastable Intermediates in the Formation of Metal–Organic Frameworks. Angewandte Chemie, 2016, 128, 2052-2056.	2.0	15
156	Effects of ECG Signal Processing on the Inverse Problem of Electrocardiography. , 2018, 45, .		15
157	Hydrothermal Synthesis of a B-Site Magnetic Ruthenate Pyrochlore. Crystal Growth and Design, 2010, 10, 3819-3823.	3.0	14
158	Disordered lithium niobate rock-salt materials prepared by hydrothermal synthesis. Dalton Transactions, 2010, 39, 6031.	3.3	14
159	High-resolution inelastic neutron scattering and neutron powder diffraction study of the adsorption of dihydrogen by the Cu(II) metal–organic framework material HKUST-1. Chemical Physics, 2013, 427, 9-17.	1.9	14
160	Exchange of Coordinated Solvent During Crystallization of a Metal–Organic Framework Observed by In Situ Highâ€Energy Xâ€ray Diffraction. Angewandte Chemie, 2016, 128, 5076-5080.	2.0	14
161	Local Aâ€Site Layering in Rareâ€Earth Orthochromite Perovskites by Solution Synthesis. Chemistry - A European Journal, 2016, 22, 18362-18367.	3.3	14
162	Time-Resolved Powder X-ray Diffraction of the Solvothermal Crystallization of Cobalt Gallate Spinel Photocatalyst Reveals Transient Layered Double Hydroxides. Chemistry of Materials, 2017, 29, 5053-5057.	6.7	14

#	Article	IF	CITATIONS
163	Structure property relationships in the ATi2O4 (A=Na, Ca) family of reduced titanates. Journal of Solid State Chemistry, 2006, 179, 3489-3499.	2.9	13
164	The effect of Mg doping on the structural and physical properties of LuFe <sub>2</sub> O <sub>4</sub> and Lu <sub>2</sub> Fe <sub>3</sub> O <sub>7</sub> . Journal of Physics Condensed Matter, 2009, 21, 015401.	1.8	13
165	Anisotropic Thermal Expansion of SiO <sub>2</sub> and AlPO <sub>4</sub> Clathrasils with the AST-Type Structure. Journal of Physical Chemistry C, 2010, 114, 6726-6733.	3.1	13
166	Structural variety in ytterbium dicarboxylate frameworks and in situ study diffraction of their solvothermal crystallisation. CrystEngComm, 2017, 19, 2424-2433.	2.6	13
167	Monitoring the Hydrothermal Growth of Cobalt Spinel Water Oxidation Catalysts: From Preparative History to Catalytic Activity. Chemistry - A European Journal, 2018, 24, 18424-18435.	3.3	13
168	Investigating discrepancies between experimental solid-state NMR and GIPAW calculation: N C–N 13C and OHâ∢O 1H chemical shifts in pyridinium fumarates and their cocrystals. Solid State Nuclear Magnetic Resonance, 2020, 108, 101662.	2.3	13
169	A furnace for the in situ study of the formation of inorganic solids at high temperature using time-resolved energy-dispersive x-ray diffraction. Review of Scientific Instruments, 2000, 71, 4177.	1.3	12
170	MIL-53(Fe): a good example to illustrate the power of powder diffraction in the field of MOFs. Zeitschrift Für Kristallographie, 2010, 225, 552-556.	1.1	12
171	Structural Characterization and Redox Catalytic Properties of Cerium(IV) Pyrochlore Oxides. Chemistry of Materials, 2011, 23, 5464-5473.	6.7	12
172	Controlled fabrication of osmium nanocrystals by electron, laser and microwave irradiation and characterisation by microfocus X-ray absorption spectroscopy. Chemical Communications, 2017, 53, 12898-12901.	4.1	12
173	Heteroatom-doped core/shell carbonaceous framework materials: synthesis, characterization and electrochemical properties. New Journal of Chemistry, 2019, 43, 5632-5641.	2.8	12
174	A zinc-based coordination polymer as adsorbent for removal of trichlorophenol from aqueous solution: Synthesis, sorption and DFT studies. Journal of Molecular Structure, 2022, 1247, 131274.	3.6	12
175	A Highly Stable Yttrium Organic Framework as a Host for Optical Thermometry and D <sub>2</sub> O Detection. Chemistry - A European Journal, 2022, 28, .	3.3	12
176	<i>In‣itu</i> timeâ€resolved Xâ€ray diffraction: The current state of the art. Synchrotron Radiation News, 2002, 15, 4-13.	0.8	11
177	Synthesis, characterization and properties of a family of lead( <scp>ii</scp> )–organic frameworks based on a multi-functional ligand 2-amino-4-sulfobenzoic acid exhibiting auxiliary ligand-dependent dehydration–rehydration behaviours. Dalton Transactions, 2014, 43, 11597-11610.	3.3	11
178	<i>In situ</i> XAFS of acid-resilient iridate pyrochlore oxygen evolution electrocatalysts under operating conditions. Physical Chemistry Chemical Physics, 2020, 22, 18770-18773.	2.8	11
179	Experimental Observations of Waterâ`Framework Interactions in a Hydrated Microporous Aluminum Phosphate. Journal of Physical Chemistry B, 2005, 109, 4464-4469.	2.6	10
180	Chapter 5 Egyptian eye cosmetics ("Kohlsâ€): Past and present. Physical Techniques in the Study of Art, Archaeology and Cultural Heritage, 2006, , 173-203.	0.3	10

#	Article	IF	CITATIONS
181	On the elastic constants of the zeolite chlorosodalite. Applied Physics Letters, 2006, 88, 021914.	3.3	10
182	Time and position resolved in situ X-ray diffraction study of the hydrothermal conversion of gypsum monoliths to hydroxyapatite. Dalton Transactions, 2009, , 8079.	3.3	10
183	Ba4Ru3O10.2(OH)1.8: a new member of the layered hexagonal perovskite family crystallised from water. Chemical Communications, 2016, 52, 6375-6378.	4.1	10
184	Synthesis and activation for catalysis of Fe-SAPO-34 prepared using iron polyamine complexes as structure directing agents. Catalysis Science and Technology, 2017, 7, 4366-4374.	4.1	10
185	Solvothermal Synthesis Routes to Substituted Cerium Dioxide Materials. Inorganics, 2021, 9, 40.	2.7	10
186	Single-crystal elastic constants of the zeolite analcime measured by inelastic X-ray scattering. Chemical Physics Letters, 2009, 471, 286-289.	2.6	9
187	<i>In situ</i> neutron diffraction study of the formation of Ho <sub>2</sub> Ge <sub>2</sub> O <sub>7</sub> pyrochlore at high temperature and pressure. Dalton Transactions, 2017, 46, 15415-15423.	3.3	9
188	Raman spectroscopy of the low-dimensional antiferromagnet <mml:math xmlns:mml="http://www.w3.org/1998/Math/MathML"&gt; <mml:mrow> <mml:msub> <mml:mi> SrRu </mml:mi> <mn mathvariant="normal"&gt;O  <mml:mn> 6 </mml:mn> </mn </mml:msub> </mml:mrow>  with large Néel temperature. Physical Review B, 2019, 99, .</mml:math 	າl:mฏ_2 <td>nml:mn&gt;</td>	nml:mn>
189	Synthesis and crystal structures of zinc(II) coordination polymers of trimethylenedipyridine (tmdp), 4-nitrobenzoic (Hnba) and 4-biphenylcarboxylic acid (Hbiphen) for adsorptive removal of methyl orange from aqueous solution. Polyhedron, 2020, 192, 114819.	2.2	9
190	Application of NMR Crystallography to Highly Disordered Templated Materials: Extensive Local Structural Disorder in the Gallophosphate GaPO-34A. Inorganic Chemistry, 2020, 59, 11616-11626.	4.0	9
191	Oxidation of 5â€Hydroxymethyl Furfural to 2,5â€Furan Dicarboxylic Acid Under Mild Aqueous Conditions Catalysed by MILâ€100(Fe) Metalâ€Organic Framework. ChemCatChem, 2022, 14, .	3.7	9
192	Open-framework fluorinated gallium and aluminium phosphates: an in situ study of the hydrothermal synthesis by X-ray diffraction using synchrotron radiation. Journal of Fluorine Chemistry, 2000, 101, 181-186.	1.7	8
193	An in situ time-resolved neutron diffraction study of the hydrothermal crystallisation of barium titanate. Chemical Communications, 2000, , 1267-1268.	4.1	8
194	Investigation of the hydrothermal crystallisation of the perovskite solid solution NaCe1â^'La Ti2O6 and its defect chemistry. Journal of Solid State Chemistry, 2013, 207, 117-125.	2.9	8
195	Investigation of some new hydro(solvo)thermal synthesis routes to nanostructured mixed-metal oxides. Journal of Solid State Chemistry, 2014, 214, 30-37.	2.9	8
196	Alkaline-Earth Rhodium Hydroxides: Synthesis, Structures, and Thermal Decomposition to Complex Oxides. Inorganic Chemistry, 2018, 57, 11217-11224.	4.0	8
197	Structures of mixed manganese ruthenium oxides (Mn <sub>1â^'x</sub> Ru <sub>x</sub> )O <sub>2</sub> crystallised under acidic hydrothermal conditions. Dalton Transactions, 2020, 49, 2661-2670.	3.3	8
198	Exploiting the flexibility of the pyrochlore composition for acid-resilient iridium oxide electrocatalysts in proton exchange membranes. Journal of Materials Chemistry A, 2021, 9, 25114-25127.	10.3	8

#	Article	IF	CITATIONS
199	Total neutron scattering investigation of the structure of a cobalt gallium oxide spinel prepared by solvothermal oxidation of gallium metal. Journal of Physics Condensed Matter, 2013, 25, 454212.	1.8	7
200	Theoretical study of conformational disorder and selective adsorption of small organic molecules in the flexible metal-organic framework material MIL-53-Fe. Molecular Simulation, 2015, 41, 1348-1356.	2.0	7
201	The intercalation of 1,10-phenanthroline into layered NiPS <sub>3</sub> <i>via</i> iron dopant seeding. Chemical Communications, 2020, 56, 4603-4606.	4.1	7
202	X-Ray absorption studies of amorphous Re2S7. Chemical Communications, 1996, , 2135.	4.1	6
203	Investigation of the solid state reaction of FeSO4·7H2O with 1,10-phenanthroline. Dalton Transactions RSC, 2002, , 3477.	2.3	6
204	Distortions of a flexible metal-organic framework from substituted pendant ligands. Acta Crystallographica Section B: Structural Science, Crystal Engineering and Materials, 2014, 70, 11-18.	1.1	6
205	<i>In Situ</i> Studies of the Crystallization of Metal-Organic Frameworks. , 0, , 729-764.		6
206	Investigating the influence of synthesis route on the crystallinity and rate capability of niobium pentoxide for energy storage. Electrochimica Acta, 2021, 392, 138964.	5.2	6
207	The ambient hydration of the aluminophosphate JDF-2 to AlPO-53(A): insights from NMR crystallography. Acta Crystallographica Section C, Structural Chemistry, 2017, 73, 191-201.	0.5	6
208	An expanded MIL-53-type coordination polymer with a reactive pendant ligand. CrystEngComm, 2018, 20, 4355-4358.	2.6	5
209	Ion-exchange resin as a new tool for characterisation of coordination compounds and MOFs by NMR spectroscopy. Chemical Communications, 2019, 55, 8106-8109.	4.1	5
210	Thermal Dehydrofluorination of GaPO-34 Revealed by NMR Crystallography. Journal of Physical Chemistry C, 2021, 125, 2537-2545.	3.1	5
211	Tuning morphology, surface, and nanocrystallinity of rare earth vanadates by one-pot colloidal conversion of hydroxycarbonates. Nanoscale, 2021, 13, 4931-4945.	5.6	5
212	The Influence of Defects on the Luminescence of Trivalent Terbium in Nanocrystalline Yttrium Orthovanadate. Nano Letters, 2022, 22, 3569-3575.	9.1	5
213	Development of New Mixed-Metal Ruthenium and Iridium Oxides as Electrocatalysts for Oxygen Evolution: Part I. Johnson Matthey Technology Review, 2022, 66, 393-405.	1.0	5
214	The synthesis and structure of a new layered aluminium phosphate [AL3P4O16]3â^' 3(CH3(CH2)3NH3)+. Studies in Surface Science and Catalysis, 1995, , 26-27.	1.5	4
215	Calcium sulfate-phosphate composites with enhanced water resistance. Journal of Materials Chemistry, 2012, 22, 4837.	6.7	4
216	Synthesis, structures and properties of a family of four two-dimensional coordination polymers constructed from 5-hydroxyisophthalate. Journal of Solid State Chemistry, 2014, 211, 8-20.	2.9	4

#	Article	IF	CITATIONS
217	Ag2Cu3Cr2O8(OH)4: a new bidimensional silver–copper mixed-oxyhydroxide with in-plane ferromagnetic coupling. Dalton Transactions, 2017, 46, 1093-1104.	3.3	4
218	A gel aging effect in the synthesis of open-framework gallium phosphates: structure solution and solid-state NMR of a large-pore, open-framework material. Dalton Transactions, 2017, 46, 16895-16904.	3.3	4
219	Nanocrystalline Transition-Metal Gallium Oxide Spinels from Acetylacetonate Precursors via Solvothermal Synthesis. Materials, 2019, 12, 838.	2.9	4
220	5â€aminoâ€2â€methylpyridinium hydrogen fumarate: An XRD and NMR crystallography analysis. Magnetic Resonance in Chemistry, 2020, 58, 1026-1035.	1.9	4
221	Synthesis, structural and DFT investigation of Zn(nba) 2 (meim) 2 for adsorptive removal of eosin yellow dye from aqueous solution. Zeitschrift Fur Anorganische Und Allgemeine Chemie, 2021, 647, 783-793.	1.2	4
222	Investigation of the preparation and reactivity of metal–organic frameworks of cerium and pyridine-2,4,6-tricarboxylate. Dalton Transactions, 2021, 51, 145-155.	3.3	4
223	An investigation of the properties of large crystals of the zeolites dodecasil-3C and ferrierite by high-temperature birefringence microscopy and X-ray diffraction. Journal of Applied Crystallography, 2010, 43, 168-175.	4.5	3
224	An investigation of Zr doping in NaBiTi <sub>2</sub> O <sub>6</sub> perovskite by direct hydrothermal synthesis. Dalton Transactions, 2015, 44, 10714-10720.	3.3	3
225	Incorporation of Sb5+ into CeO2: local structural distortion of the fluorite structure from a pentavalent substituent. Dalton Transactions, 2018, 47, 9693-9700.	3.3	3
226	Electric Field ontrolled Synthesis and Characterisation of Single Metal–Organicâ€Framework (MOF) Nanoparticles. Angewandte Chemie, 2020, 132, 19864-19869.	2.0	3
227	Hydrothermal Synthesis of Iridium-Substituted NaTaO3 Perovskites. Nanomaterials, 2021, 11, 1537.	4.1	3
228	Study of The Hydrothermal Synthesis of Gallium Phosphates Using in Situ Time-Resolved X-Ray Diffraction. Materials Research Society Symposia Proceedings, 1998, 547, 63.	0.1	1
229	The Structure of Amorphous CrS3 Containing [CrIII2((Sâ^'I)2)3]x Chains: An X-Ray Diffraction Modeling Study, Journal of Solid State Chemistry, 1999, 145, 573-579, Observation of two O-H covalent bonds of water in the smml:math	2.9	1
230	xmlns:mml="http://www.w3.org/1998/Math/MathML" display="inline"> <mml:mrow><mml:msub><mml:mi mathvariant="normal"&gt;Na<mml:mn>0.3</mml:mn></mml:mi </mml:msub><mml:mi mathvariant="normal"&gt;Co<mml:msub><mml:mi mathvariant="normal"&gt;O<mml:mn>2</mml:mn></mml:mi </mml:msub><mml:mo>â^™</mml:mo><mml:mn>1</mml:mn></mml:mi </mml:mrow>	3.2 3 <td>1 1n&gt;<mml:msu< td=""></mml:msu<></td>	1 1n> <mml:msu< td=""></mml:msu<>
231	mathvariant="normal">H <mml:mn>2</mml:mn> <mml:mi mathvariant="normal"&gt; Microstructure and oxidation states in multiferroic Lu2(Fe,Mn)307. Journal of Applied Physics, 2012, 112, .</mml:mi 	2.5	1
232	Structural Disorder in (Bi, M)2(Fe, Mn, Bi)2O6+x (M = Na or K) Pyrochlores Seen from Reverse Monte Carlo Analysis of Neutron Total Scattering. Journal of Physical Chemistry C, 2017, 121, 18120-18128.	3.1	1
233	Ce(OH)2Cl and lanthanide-substituted variants as precursors to redox-active CeO2 materials. Dalton Transactions, 2020, 49, 14871-14880.	3.3	1
234	Crystallization of a Large-Pore Three-Dimensional Gallium Fluorophosphate under Mild Conditions. Angewandte Chemie - International Edition, 2000, 39, 4552-4555.	13.8	1

#	Article	IF	CITATIONS
235	An Investigation of the Synthesis of the Layered Perovskite RbCa2Nb3O10Using Time-Resolved in situ High-Temperature Powder X-Ray Diffraction ChemInform, 2003, 34, no-no.	0.0	0
236	Subcritical Hydrothermal Synthesis of Perovskite Manganites: A Direct and Rapid Route to Complex Transition-Metal Oxides ChemInform, 2003, 34, no.	0.0	0
237	Probing Molten Salt Flux Reactions Using Time-Resolved in situ High-Temperature Powder X-Ray Diffraction: A New Synthesis Route to the Mixed-Valence NaTi2O4 ChemInform, 2004, 35, no.	0.0	0
238	Investigation of Hydrothermal Routes to Mixed-Metal Cerium Titanium Oxides and Metal Oxidation State Assignment Using XANES ChemInform, 2004, 35, no.	0.0	0
239	Development of freeze flow apparatus to study filled polymer melts. Polymer Engineering and Science, 2007, 47, 1937-1942.	3.1	0
240	Controlled Hydrothermal Synthesis of Complex Mixed Oxides Using Solution Redox Chemistry. Materials Research Society Symposia Proceedings, 2011, 1309, 67.	0.1	0
241	Introduction to the special issue on energy materials. Acta Crystallographica Section B: Structural Science, Crystal Engineering and Materials, 2015, 71, 583-584.	1.1	0
242	Frontispiece: Monitoring the Hydrothermal Growth of Cobalt Spinel Water Oxidation Catalysts: From Preparative History to Catalytic Activity. Chemistry - A European Journal, 2018, 24, .	3.3	0
243	Frontispiece: Perovskite Oxides Prepared by Hydrothermal and Solvothermal Synthesis: A Review of Crystallisation, Chemistry, and Compositions. Chemistry - A European Journal, 2020, 26, .	3.3	0
244	Isolated zirconium centres captured from aqueous solution: the structure of zirconium mandelate revealed from NMR crystallography. Chemical Communications, 2020, 56, 10159-10162.	4.1	0
245	Ga2.52V2·48O7·33(OH)0.67, a synthetic member of the nolanite/akdalaite-type family of oxyhydroxides containing trivalent vanadium. Journal of Solid State Chemistry, 2020, 288, 121396.	2.9	0
246	Doped Manganites. , 2008, , 95-102.		0
247	Calcium coordination compounds of anionic forms of hydrogen dipicolinate and quinolinate: synthesis, characterization, crystal structures and DFT studies. Structural Chemistry, 0, , 1.	2.0	0